Chemical Science

Accepted Manuscript

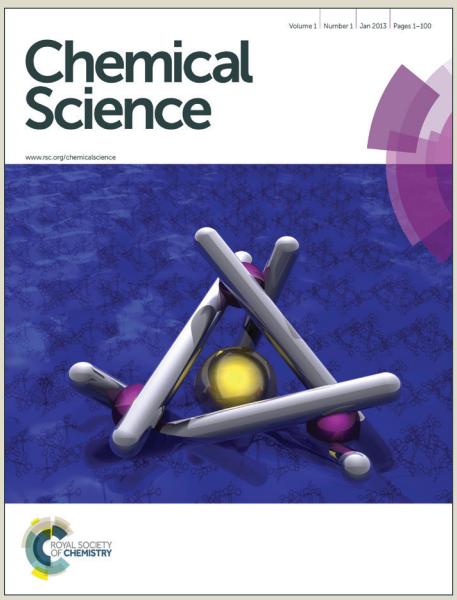

ROYAL SOCIETY OF CHEMISTRY

www.rsc.org/chemicalscience

Journal Name

RSCPublishing

ARTICLE

Time-Resolved Botulinum Neurotoxin A Activity Monitored using Peptide-Functionalized Au Nanoparticle Energy Transfer Sensors†

Yi Wang,[a,b] Xiaohu Liu,[a] Jinling Zhang,[a,b] Daniel Aili,[a,c] Bo Liedberg*[a,b]

Cite this: DOI: 10.1039/x0xx00000x

Received 00th January 2012,
Accepted 00th January 2012

DOI: 10.1039/x0xx00000x

www.rsc.org/

We report herein on the employment of synthetic peptide-functionalized gold nanoparticles (AuNPs) with various diameters as radiative quenchers for the time-resolved monitoring of botulinum A light chain (BoLcA) activity. The results demonstrate that large AuNPs provided higher energy transfer efficiency between the dye and the AuNPs, but poorer BoLcA activity for proteolysis of peptides because of the steric constraints. The initial turnover number for the BoLcA proteolysis of peptides on 18 nm AuNPs was retarded by a factor of 80 as compared with 1.4 nm AuNPs. A similar phenomenon has been observed for trypsin, however, with less hindrance on the large AuNPs. Thus, the use of small 1.4 nm AuNPs in conjunction with robust synthetic peptides provides an attractive format for time-resolved monitoring of protease activity and for BoLcA sensing at a highly competitive limit of detection (1 pM).

Introduction

Botulinum neurotoxins (BoNTs), produced by Clostridium botulinum,[1] are considered the most lethal substance known to humans. BoNTs are classified into seven immunologically distinct serotypes (A-G) each of which can cause flaccid muscle paralysis and subsequent death by blocking the release of neurotransmitters at neuromuscular junctions. Structurally, the neurotoxins are expressed as a single chain polypeptide which after post-translational proteolysis consists of two subunits: a 100 kDa heavy chain (HC) and a 50 kDa light chain (LC) linked via a disulfide bond. The HC is responsible for the binding and translocation of the toxin across the synaptic membrane through specific receptors; whereas the LC function as an active zinc-endopeptidase that cleaves the SNARE proteins (soluble N-ethylmaleimide-sensitive factor attachment protein receptor) leading to inhibition of acetylcholine release and subsequent neuroparalysis.[2] The neurotoxin can enter the body via the gastrointestinal tract or through mucous membranes of, for instance, the eyes or the respiratory tract. In human, a lethal dose intravenously is estimated at 1-2 ng/kg body weight, orally at 1 μg/kg and 10-12 ng/kg by inhalation.[3] The gold standard "mouse bioassay" is able to detect as little as 10 pg/ml of toxin,[4] however, it requires several days of assay time, large number of animals and can only be performed at specific laboratories. Therefore rapid, sensitive and easily accessible assays are required to meet biodefense diagnostic and therapeutic needs.

A number of *in vitro* assays to detect BoNTs, including ELISA,[5] immuno-PCR,[6] surface plasmon resonance (SPR) immunoassay[7] and electrochemical luminescence[8] have been developed.[9] However, these assays usually do not provide information on the enzymatic activity that is responsible for the toxicity of BoNTs. By rational design of a peptide substrate containing the BoNTs cleavage site derived from the SNARE protein, it is possible to monitor the activity of various serotypes of BoNTs as each serotype cleaves at different sites of the SNARE protein. Assays to monitor the activity of BoNTs are typically based on measuring the mass changes after the cleavage of the substrate via SPR;[10] counting the number of amplifiers or labels such as phages-based amplifiers,[11] or monitoring the reduction in the fluorescence resonance energy transfer (FRET) upon the cleavage of substrates.[12] Among these methods FRET has been extensively applied for monitoring proteolytic activities of various proteases including trypsin, caspase 1, caspase 3, thrombin, chymotrypsin, collagenase, HIV-1 protease and so on.[13] Several of the organic fluorophores commonly used in FRET bioassays suffer from pH sensitivity, photo-bleaching, chemical degradation and absorption spectra overlapping between the acceptor and donor. To address these problems, quantum dots (QDs) have been employed in FRET because of their relative stability, tuneable emissions for optimizations of the spectra overlap with a particular acceptor, and potential minimization of the direct acceptor excitation.[14] However, the overlapping emission between the donor and acceptor is still unavoidable in addition to the potential toxicity of QDs.[15] Accordingly, having an acceptor that is non-fluorescent, such as metallic nanoparticles, can help to solve these issues. Metal nanoparticles have found applications either as radiative quenchers or radiative enhancers, depending on the

particle size, shape, composition, and the distance between the donor and metal nanoparticle.[16] For Au nanoparticles smaller than 40 nm in diameter, the absorption term dominates over scattering, and radiative quenching becomes the main cause for energy transfer from the dye to the metal which results in electron-hole pair formations and subsequent Ohmic losses.[16a] On the contrary, large nanoparticles are expected to enhance the fluorescence because scattering dominates over absorption. Au nanoparticles have been utilized before as quenching beacons for the detection of DNA,[17] RNA,[18] proteases[19] and other biomolecules.[20]

In this paper, Au nanoparticles with diameter of 1.4 nm, 6 nm and 18 nm were modified with peptides containing a BoLcA cleavage site (AuNP-pep) and employed as radiative quenchers for monitoring the activity of BoLcA. The AuNP-pep construct was pre-treated (cleaved) with BoLcA prior to the incubation with the streptavidin-Alexa 488 conjugate (SA488) for the measurement of the fluorescence intensity, Fig.1. The fluorescence energy transfer efficiency was first investigated for AuNPs of different sizes. Then, the time-resolved catalytic activity of BoLcA on AuNP-pep constructs was monitored and compared with the activity of trypsin on the same AuNP-pep construct. Finally, we employed the assay format in Fig. 1 for BoLcA sensing.

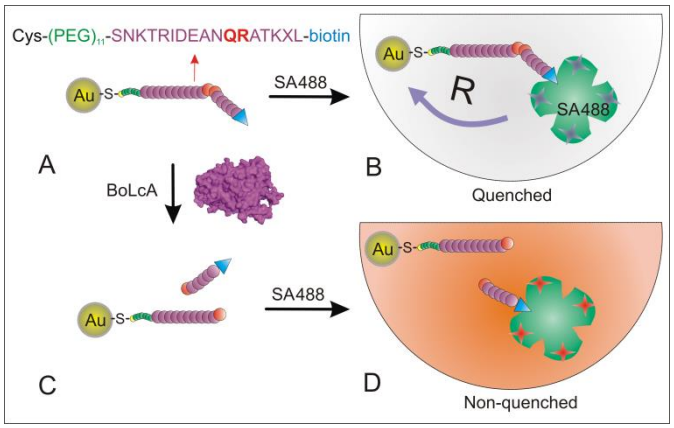

Fig. 1 Scheme showing the energy transfer between peptide-functionalized AuNP and streptavidin-Alexa488 (SA488) before and after catalytic cleavage by BoLcA. (A) 1.4 nm AuNPs functionalized with peptide substrate containing the BoLcA cleavage site (QR) and a terminal biotin. (B) Quenching of SA488 caused by the short distance R between dye and the AuNP surface. (C) Cleavage of peptide on AuNP by BoLcA. (D) Addition of SA488 to the suspension of the peptide-functionalized AuNPs after BoLcA cleavage.

Results and discussion

Peptide sequence

Previous research has reported that a short peptide derived from the C-terminal end (187-203) of the SNAP-25 protein (part of the SNARE complex) can be hydrolyzed by BoNT at a similar rate as the full length SNAP-25, as long as the peptide has a minimum length of 14 to 16 amino acids and that arginine is present at the cleavage site.[21] The peptide sequence used in our study was designed based on the 17 amino acids at the C-terminus of SNAP-25 protein (187-203). The glutamine-arginine (Q-R) located in the middle of the target peptide is the cleavage site for BoLcA proteolysis according to mass spectrometer results (Fig. S1†) and previous work.[21-22] Further, substitution of methionine (M) in position 202 with norleucine (X) increases the proteolytic rate of BoLcA.[21, 23] At the N-terminus of the peptide a cysteine was attached to enable immobilization on AuNPs via the -SH moiety.[24] In addition, an 11 unit ethylene glycol oligomer was introduced as a spacer between Cys and the recognition sequence to minimize the steric hindrance caused by AuNPs. At the C-teriminus a biotin molecule was added for the specific interaction with the streptavidin-dye conjugate. The SA488 contains 3-6 dyes per proteins (see ESI†), which is advantageous compared with a single-dye labelled peptide, as it provides higher fluorescence response to the peptide-cleavage induced dye release.

AuNP size-dependent energy transfer efficiency

The peptide was attached to AuNPs with sizes of 1.4, 6 and 18 nm in diameter, see experimental details in ESI† and Fig. S2†, and their respective extinction spectra are shown in Fig. 2A. The 1.4 nm AuNPs display significantly less extinction as compared with the 6 nm and 18 nm AuNPs because of its small electron density at the conduction band and large damping.[25] The 1.4 nm AuNP modified with the peptide substrate (AuNP-pep) was then incubated with SA488 at different molar ratios AuNP-pep/SA488. The fluorescence intensity at λ = 520 nm decreased from I_0=5.45×10^5 cps/μA for 10 nM SA488 to I'=2.0×10^5 cps/μA upon increasing the molar ratio of AuNP-pep/SA488 to 20:1 (Fig. 2B), and the energy transfer efficiency E=1-I'/I_0 saturated at 62.5% for a AuNP-pep/SA488 ratio ≥ 5 (Fig. 2C). The maximum fluorescence quenching efficiency was observed for a AuNP-pep/SA488 ratio of ~5 which is reasonable given that streptavidin has 4 affinity binding sites for biotins. Previous work suggests that small AuNPs with the diameter of ~1-3 nm as an acceptor can be described by the nanometal surface energy transfer (NSET) theory.[16a] In contrast to FRET, NSET does not require a resonant electronic transition as it originates from the interaction of the electromagnetic field of the donor dipole with the free conduction electrons of the accepting metal. The NSET characteristic distance R_0 is expressed as

$$R_0 = \left(0.225 \frac{c^3 \Phi_D}{\omega^2 \omega_f k_f} \right)^{1/4} \quad (1)$$

where Φ_D is the donor quantum efficiency, ω is the frequency of the donor electronic transition, ω_f and k_f are the Fermi frequency and Fermi wavevector of Au, respectively. In general, the fluorescence quenching efficiency E can be expressed as a function of the donor/acceptor distance, R, as

$$E = \frac{1}{1+(R/R_0)^n} \quad (2)$$

where n = 6 for FRET and n = 4 for NSET. The NSET radius (R_0) is calculated to equal R_0 = 7.78 nm, according to Eq. (1) by using quantum efficiency of Alexa Fluor 488 Φ_D = 0.8, ω = 3.63×10^{15} s^{-1}, ω_f = 8.4×10^{15} s^{-1} and k_f = 1.2×10^8 cm^{-1}. Note that R is the distance between the molecular donor center and Au surface for NSET, while for FRET, R is the distance between the donor center and the center

of Au nanoparticles. The distance dependent fluorescence quenching efficiency (Eq. (2)) is plotted in Fig. 2D, from which the distance between the dye and AuNPs was estimated as R = 6.85 nm in the case of 1.4 nm AuNP-pep constructs based on NSET. The distance is shorter than the linear extension length of the peptide L ~ 8 nm which might indicate that the immobilized peptide adopts a slightly bended or folded structure.

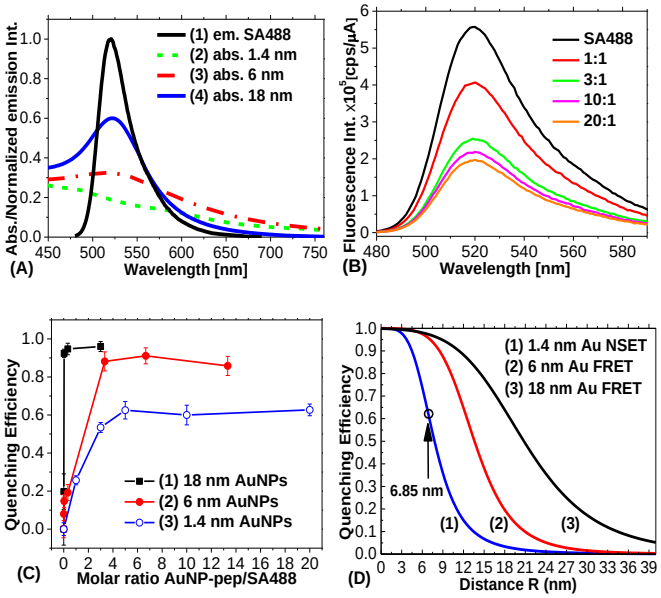

Fig. 2 (A) Normalized emission spectrum of (1) SA488 and absorption spectra of (2) 1.4 nm, (3) 6 nm and (4) 18 nm AuNP-pep. (B) Fluorescence spectra of 10 nM SA488 and its incubation with 1.4 nm AuNP-pep at AuNP-pep/SA488 ratio from 1:1 to 20:1. (C) Fluorescence quenching efficiency plotted as the function of the molar ratio of AuNP-pep/SA488 with the AuNPs diameter of (1) 18 nm, (2) 6 nm and (3) 1.4 nm. (D) Simulated fluorescence quenching efficiency versus the distance between the dyes and the surface of the AuNPs with a diameter of (1) 1.4 nm, (2) 6 nm and (3) 18 nm based on NSET, FRET and FRET, respectively.

As compared with 1.4 nm AuNPs, the larger AuNPs, with diameter of 6 nm and 18 nm, displayed an increasing fluorescence quenching efficiency (Fig. 2C). The fluorescence quenching efficiency for 6 nm and 18 nm AuNPs reached a maximum at around 90% and 98% for molar ratios of 3:1 and 1:3, respectively. This is reasonable as the large AuNPs offer higher extinction coefficient and carry a larger number of peptide. The 1.4 nm AuNP was modified with single maleimide group for attachment of one peptide per AuNP (see ESI†). The average number of peptides on each 18 nm and 6 nm AuNPs was estimated to be 51 and 3, respectively. This estimation is based on a peptide/thiol-PEG molar ratio of 1:100 (18 nm AuNPs) and 0.5:100 (6 nm AuNPs), respectively, and the assumption that each thiol occupies an area of 0.2 nm^2. These observations in Fig. 2 suggest that the fluorescence quenching efficiency is determined by both the size of the AuNPs, and the coverage of peptides on the AuNPs. The fluorescence quenching efficiency reached the maximum at a relatively lower AuNP-pep/SA488 ratio when increasing the coverage of peptide on 6 nm AuNPs (Fig. S3†). Furthermore, the energy transfer for large AuNPs with diameter of 6 nm and 18 nm were assumed to be dominated by FRET, from which the characteristic radius (R_0) is estimated as R_0 = 16.6 and 29.8 nm, respectively (see ESI†). Accordingly, based on the calculation that the distance between the dye and the AuNPs surface is about R = 6.85 nm, we estimate a quenching efficiency of E~95% and 98% for the 6 and 18 nm AuNPs, respectively (Eq. (2)). These values are consistent with the maximum fluorescence quenching efficiencies of E=92% and 98% for the 6 and 18 nm AuNPs, respectively, as presented in Fig. 2C. Thus, our results confirm that the energy transfer on AuNPs with a diameter larger than 6 nm follows the FRET mechanism. One can of course argue that there is always a risk for aggregation between AuNPs induced by the multivalency of streptavidin (4 binding pockets/molecule). This might occur when there is more than one peptide/AuNP (as for the 6 and 18 nm particles). However, no colour change nor any plasmon band shift were observed after mixing SA488 with 6 nm AuNP at the molar ratio AuNP-pep/SA488 of 3:1, indicating negligible aggregation of AuNPs (Fig. S4†).

AuNPs size-dependent protease activity

The BoLcA activity was monitored through time-dependent fluorescence spectra of SA488 incubated with 1.4 nm AuNP-peps which were pre-treated with BoLcA for 30 min up to 6 hours (Fig. 3A). The fluorescence intensity at the emission wavelength of 520 nm increased from 2.2×10^5 to 3.2×10^5 cps/μA after 0.5 h incubation with 10 nM BoLcA and reached saturation at 4.0×10^5 cps/μA after 2 h incubation.

The time-dependent peptide cleavage for AuNPs with diameter 1.4 nm, 6 nm and 18 nm is demonstrated in Fig. 3B. The kinetics show saturation in 2 to 5 hours for the 1.4 nm AuNP-pep (200 nM) after exposure to 3 nM and 10 nM BoLcA, with the initial catalytic rate v = 0.6 nM min^{-1} and 2 nM min^{-1}, respectively. This corresponds to an initial turnover number of k = 0.2 min^{-1}. The corresponding initial turnover number for 6 nm and 18 nm AuNPs is 0.0025 min^{-1}, which is 80-fold lower than that for the 1.4 nm AuNPs. The k values were calculated based on a coverage of 3 peptides per 6 nm AuNP (12 nM) and 51 peptides per 18 nm AuNP (1 nM) which were cleaved initially at a rate of 0.78 and 0.75 peptide per hour with 5 nM BoLcA, respectively. The rate constant is calculated as $K_T = k_{cat}/K_M$ to equal 2.8×10^6 M^{-1} min^{-1} (see Fig. 3D and details in ESI†), based on the fitting of the kinetics on 1.4 nm AuNP-pep incubation with 3 nM and 10 nM BoLcA. Assuming the k_{cat} = 30 s^{-1} as reported with the same peptide sequence,[21] the Michaelis-Menten constant K_M is estimated to equal K_M = 643 μM, which is comparable to that of the free peptide.[21] The poorer activity of BoLcA for the peptide on large AuNPs is ascribed to the fact that the active pocket of BoLcA is deeply buried inside the enzyme (~2.4 nm)[26], and steric hindrance induced by the AuNPs.

A similar phenomenon was also observed for trypsin and the same AuNP-pep. The catalytic rate of trypsin is higher on small AuNPs than on large AuNPs as indicated in Fig. 3C. The cleavage percentage was defined as $\Delta F/(F_{SA488}-F_0)$, where F_{SA488} and F_0 are the fluorescence intensities of free SA488 and AuNP-pep-SA488 conjugates measured at λ=520 nm, respectively. The results indicated that about 90% of peptides on AuNPs were hydrolyzed by trypsin in 1, 4 and 10 hours for 1.4 nm, 6 nm and 18 nm AuNP-pep,

respectively. As compared with BoLcA (Fig. 3B), trypsin hydrolyze a higher amount of peptide in shorter reaction time, indicating a higher activity. The rate constant K_T was accordingly estimated as K_T = 8.1×10^7 M^{-1} min^{-1}, 7.2×10^6 M^{-1} min^{-1} and 4.42×10^6 M^{-1} min^{-1} on the AuNPs with diameter of 1.4 nm, 6 nm and 18 nm, respectively (Fig. 3D). The K_T values are comparable to previously reported values 7.8×10^7 - 2.34×10^8 M^{-1} min^{-1} for trypsin digesting a fifteen-residue peptide substrate,[27] but 3 orders of magnitude higher than that reported for four-residue peptide substrates containing an arginine cleavage site.[28] The trypsin proteolytic activity is about 29 times higher than that of BoLcA. Furthermore, upon increasing the size of AuNPs from 1.4 nm to 18 nm in diameter, the trypsin activity was decreased by 18 fold, a decrease that is 4 times smaller as compared with the 80-fold decrease for BoLcA (Fig. 3D). Again the poor catalytic activity of BoLcA and more significant hindrance by large AuNPs might be ascribed to the deeper active pocket sites and 2-fold higher molecular weight of BoLcA as compared to trypsin, as well as the smaller number of cleavage sites provided by the peptide substrate. There are in total 4 trypsin cleavage sites (i.e. lysine K and arginine R) and only one (QR) for BoLcA.

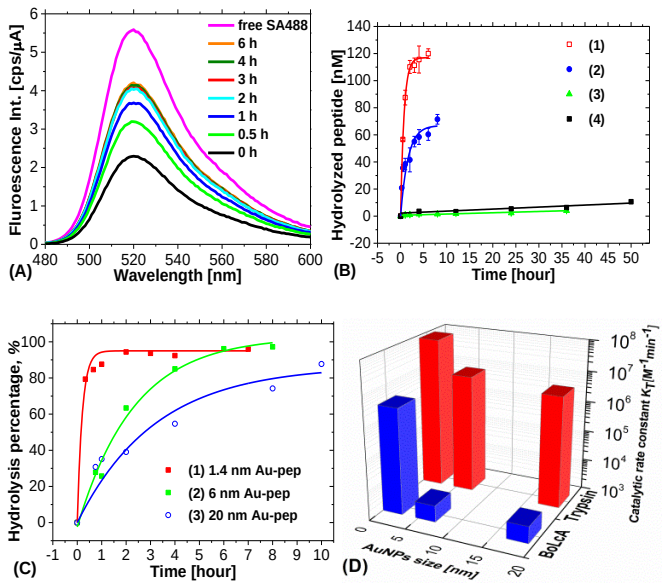

Fig. 3 (A) Evolution of the fluorescence intensity upon SA488 interaction with 1.4 nm AuNP-pep pre-incubated with 10 nM BoLcA for 0 to 6 hours at 37 ℃. (B) The time-dependent evolution of peptide hydrolysis measured on 1.4 nm AuNP-pep treated with (1) 10 nM BoLcA and (2) 3 nM BoLcA, (3) 6 nm and (4) 18 nm AuNP-pep treated with 5 nM BoLcA, respectively. (C) The time-dependent evolution of peptide hydrolysis measured on (1) 1.4 nm, (2) 6 nm and (3) 18 nm AuNP-pep which were pretreated with 1 nM trypsin. (D) The size-dependent protease rate constant K_T of trypsin and BoLcA on 1.4 nm, 6 nm and 18 nm AuNP-pep.

BoLcA sensing

Considering the situation that the large AuNPs significantly hindered the accessibility of BoLcA to the peptides on the surface, we employed the smallest AuNPs (i.e. 1.4 nm in diameter) for the detection of BoLcA. The time-dependent fluorescence intensity of SA488 was monitored after incubation with AuNP-pep which was pre-treated with BoLcA at various concentrations from 1 pM to 10 nM at 37 ℃ (Fig. 4A). The fluorescence intensity saturated quickly after 2 hours incubation of AuNP-pep with BoLcA at concentrations higher than 3 nM (Fig. 4A). However, at low concentration of BoLcA (< 3nM), the fluorescence intensity increased approximately at a near linear speed after 2 hours incubation. It is interesting to notice that at concentrations of BoLcA lower than 3 nM the fluorescence intensity decreased in the first reaction hour (see insert in Fig. 4A). This might tentatively be ascribed to a transient conformational change of the peptide upon affinity interaction with BoLcA prior to cleavage. This hypothesis is based on the assumption that the fluorescence decline is due to a distance decrease between the dye and the AuNP. The same trend was not observed for trypsin at concentrations down to 1 pM because of its high catalytic rate and its less deep catalytic/cleavage site as compared with BoLcA (Fig. 3D, 4A). However, to confirm that the peptide changes conformation upon affinity interaction with BoLcA requires more advanced single-molecule measurements,[29] experiments that are beyond the scope of the present study.

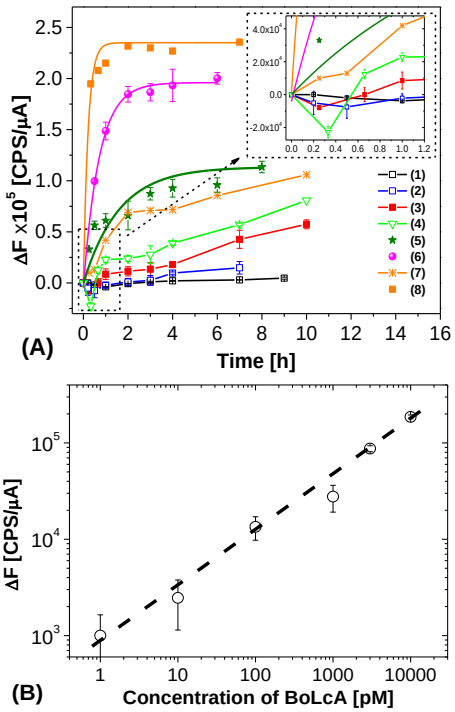

Fig. 4 (A) The time-dependent fluorescence intensity changes ΔF of SA488 on 1.4 nm AuNP-pep pretreated with (1) 1 pM, (2) 10 pM, (3) 100 pM, (4) 1 nM, (5) 3 nM, (6) 10 nM BoLcA and (7) 10 pM and (8) 1 nM trypsin, respectively. (B) The calibration curve for the detection of BoLcA corresponding to the response at 2 hour incubation of the kinetics in A.

The calibration curve for the BoLcA from 1 pM to 10 nM reveals a limit of detection (LOD) of 1 pM (50 pg/ml), which is determined as the concentration of BoLcA at which the fluorescence intensity changes ΔF is three times of the standard deviation of the fluorescence fluctuation of control samples, i.e. 3×δF=1000 cps/μA. The method provided sensitive detection of BoLcA with the assay time of 2-3 hours which is comparable to the vesicle amplified SPR

sandwich assay (LOD ~0.3 to 10 pM and assay time from 10 min to several hours)[10], aptamber-based electrochemical assay (LOD of 40 pg/ml and assay time of 24 h)[30], and the antibody-based SPR sandwich assay on the detection of BoNT Type B in buffer and honey (LOD~ 2 pM and assay time of 1-2 h)[7]. The LOD is about 2 to 3 orders of magnitude lower than the quantum dots based FRET method (LOD ~ 350 pM and assay time of 2-3 h)[31], antibody-based ELISA (LOD of 0.2-2 ng/ml and assay time of 8 h)[5]. But it is less sensitive than mouse lethality assay (LOD of 20-30 pg/ml and assay time of 2-4 days)[32]. However, our method typically provides shorter assay time than conventional ELISA and mouse lethality assay, it is expected to be more robust assay as compared with the antibody-based assays.

Conclusion

We have designed and synthesized a substrate peptide, which was immobilized on AuNPs with diameter of 1.4-18 nm for the detection of BoLcA activity using a fluorescence energy transfer assay format. The results indicated that large AuNPs provided higher quenching efficiency, but significantly hindered the accessibility of BoLcA to the peptides on the AuNPs surface thus leading to an 80-fold lower initial catalytic rate of BoLcA. The assay provided limit of detection (LOD) of 1 pM for the detection of BoLcA with the assay time of 2-3 hours which is faster and more sensitive than many other assays including conventional ELISA. The proposed assay based on synthetic peptide is also more robust than antibody-based assays.

Acknowledgements

This research is supported by Science & Engineering Research Council (SERC) of Agency for Science, Technology and Research (A*STAR), for projects under the numbers of 102 152 0015**.**

Notes

[a] *Centre for Biomimetic Sensor Science, Nanyang Technological University, 50 Nanyang Avenue, 637553 Singapore. Tel: 65 6316 2957; E-mail: bliedberg@ntu.edu.sg*
[b] *School of Materials Science and Engineering, Nanyang Technological University, 50 Nanyang Avenue, 639798 Singapore.*
[c] *Division of Molecular Physics, Department of Physics, Chemistry and Biology, Linköping University, 58183 Linköping, Sweden*

† Electronic Supplementary Information (ESI) available: Details of Experiments, FRET calculation, MALDI-TOF, DLS characterization and peptide-ratio dependent quenching efficiency of AuNPs. See DOI: 10.1039/b000000x/

References

1. C. Montecucco and J. Molgo, *Curr. Opin. Pharmacol.*, 2005, **5**, 274-279.
2. (a) B. R. Singh, *Neurotox. Res.*, 2006, **9**, 73-92; (b) G. Schiavo, M. Matteoli and C. Montecucco, *Physiol. Rev.*, 2000, **80**, 717-766; (c) L. Li and B. R. Singh, *J. Toxicol-Toxin Rev.*, 1999, **18**, 95-112.
3. S. S. Arnon, R. Schechter, T. V. Inglesby, D. A. Henderson, J. G. Bartlett, M. S. Ascher, E. Eitzen, A. D. Fine, J. Hauer, M. Layton, S. Lillibridge, M. T. Osterholm, T. O'Toole, G. Parker, T. M. Perl, P. K. Russell, D. L. Swerdlow, K. Tonat and W. G. C. Biodefense, *Jama-J. Am. Med. Assoc.*, 2001, **285**, 1059-1070.
4. S. K. Sharma and R. C. Whiting, *J. Food Prot.*, 2005, **68**, 1256-1263.
5. (a) M. A. Poli, V. R. Rivera and D. Neal, *Toxicon*, 2002, **40**, 797-802; (b) M. Szilagyi, V. R. Rivera, D. Neal, G. A. Merrill and M. A. Poli, *Toxicon*, 2000, **38**, 381-389.
6. (a) J. T. Mason, L. X. Xu, Z. M. Sheng and T. J. O'Leary, *Nat. Biotechnol.*, 2006, **24**, 555-557; (b) J. T. Mason, L. Xu, Z. M. Sheng, J. He and T. J. O'Leary, *Nat. Protoc.*, 2006, **1**, 2003-2011; (c) H. C. Wu, Y. L. Huang, S. C. Lai, Y. Y. Huang and M. F. Shalo, *Lett. Appl. Microbiol.*, 2001, **32**, 321-325.
7. J. Ladd, A. D. Taylor, J. Homola and S. Y. Jiang, *Sensor. Actuat. B-Chem.*, 2008, **130**, 129-134.
8. (a) V. R. Rivera, F. J. Gamez, W. K. Keener, J. A. White and M. A. Poli, *Anal. Biochem.*, 2006, **353**, 248-256; (b) V. Guglielmo-Viret, O. Attree, V. Blanco-Gros and P. Thullier, *J. Immunol. Methods*, 2005, **301**, 164-172.
9. J. W. Grate, R. M. Ozanich, M. G. Warner, J. D. Marks and C. J. Bruckner-Lea, *Trac-Trend. Anal. Chem.*, 2010, **29**, 1137-1156.
10. G. Ferracci, S. Marconi, C. Mazuet, E. Jover, M. P. Blanchard, M. Seagar, M. Popoff and C. Leveque, *Anal. Biochem.*, 2011, **410**, 281-288.
11. P. Capek, K. S. Kirkconnell and T. J. Dickerson, *J. Am. Chem. Soc.*, 2010, **132**, 13126-13128.
12. (a) S. Sun, J. Francis, K. E. Sapsford, Y. Kostov and A. Rasooly, *Sensor. Actuat. B-Chem.*, 2010, **146**, 297-306; (b) D. Min, W. H. Tepp, E. A. Johnson and E. R. Chapman, *Proc. Natl. Acad. Sci. U. S. A.*, 2004, **101**, 14701-14706; (c) J. J. Schmidt, R. G. Stafford and C. B. Millard, *Anal. Biochem.*, 2001, **296**, 130-137; (d) J. A. Ross, M. A. Gilmore, D. Williams, K. R. Aoki, L. E. Steward and D. M. Jameson, *Anal. Biochem.*, 2011, **413**, 43-49.
13. (a) Y. Choi, J. Lee, K. Kim, H. Kim, P. Sommer and R. Song, *Chem. Commun.*, 2010, **46**, 9146-9148; (b) Y. H. Wang, P. Shen, C. Y. Li, Y. Y. Wang and Z. H. Liu, *Anal. Chem.*, 2012, **84**, 1466-1473; (c) T. Zauner, R. Berger-Hoffmann, K. Muller, R. Hoffmann and T. Zuchner, *Anal. Chem.*, 2011, **83**, 7356-7363; (d) J. Karvinen, V. Laitala, M. L. Makinen, O. Mulari, J. Tamminen, J. Hermonen, P. Hurskainen and I. Hemmila, *Anal. Chem.*, 2004, **76**, 1429-1436; (e) D. E. Prasuhn, A. Feltz, J. B. Blanco-Canosa, K. Susumu, M. H. Stewart, B. C. Mei, A. V. Yakovlev, C. Loukov, J. M. Mallet, M. Oheim, P. E. Dawson and I. L. Medintz, *ACS Nano*, 2010, **4**, 5487-5497.
14. (a) I. L. Medintz, A. R. Clapp, F. M. Brunel, T. Tiefenbrunn, H. T. Uyeda, E. L. Chang, J. R. Deschamps, P. E. Dawson and H. Mattoussi, *Nat. Mater.*, 2006, **5**, 581-589; (b) K. Boeneman, B. C. Mei, A. M. Dennis, G. Bao, J. R. Deschamps, H. Mattoussi and I. L. Medintz, *J. Am. Chem. Soc.*, 2009, **131**, 3828-+; (c) H. Q. Yao, Y. Zhang, F. Xiao, Z. Y. Xia and J. H. Rao, *Angew. Chem., Int. Ed.*, 2007, **46**, 4346-4349; (d) L. F. Shi, V. De Paoli, N. Rosenzweig and Z. Rosenzweig, *J. Am. Chem. Soc.*, 2006, **128**, 10378-10379; (e) W. R. Algar, A. Malonoski, J. R. Deschamps, J. B. Banco-Canosa, K. Susumu, M. H. Stewart, B. J. Johnson, P. E. Dawson and I. L. Medintz, *Nano Lett.*, 2012, **12**, 3793-3802.
15. (a) R. Hardman, *Environ. Health Perspect.*, 2006, **114**, 165-172; (b) M. Bottrill and M. Green, *Chem. Commun.*, 2011, **47**, 7039-7050; (c) L. Y. T. Chou and W. C. W. Chan, *Nat. Nanotechnol.*, 2012, **7**, 416-417.
16. (a) M. P. Singh and G. F. Strouse, *J. Am. Chem. Soc.*, 2010, **132**, 9383-9391; (b) T. L. Jennings, M. P. Singh and G. F. Strouse, *J. Am. Chem. Soc.*, 2006, **128**, 5462-5467; (c) J. R. Lakowicz, *Anal. Biochem.*, 2005, **337**, 171-194; (d) T. Pons, I. L. Medintz, K. E. Sapsford, S. Higashiya, A. F. Grimes, D. S. English and H. Mattoussi, *Nano Lett.*, 2007, **7**, 3157-3164; (e) Y. Wang, L. Wu, X. D. Zhou, T. I. Wong, J. L. Zhang, P. Bai, E. P. Li and B. Liedberg, *Sensor. Actuat. B-Chem.*, 2013, **186**, 205-211.
17. (a) B. Dubertret, M. Calame and A. J. Libchaber, *Nat. Biotechnol.*, 2001, **19**, 365-370; (b) H. Wang, J. S. Li, Y. X. Wang, J. Y. Jin, R. H. Yang, K. M. Wang and W. H. Tan, *Anal. Chem.*, 2010, **82**, 7684-7690; (c) F. Li, H. Pei, L. H. Wang, J. X. Lu, J. M. Gao, B. W. Jiang, X. C. Zhao and C. H. Fan, *Adv. Funct. Mater.*, 2013, **23**, 4140-4148.
18. (a) D. S. Seferos, D. A. Giljohann, H. D. Hill, A. E. Prigodich and C. A. Mirkin, *J. Am. Chem. Soc.*, 2007, **129**, 15477-+; (b) J. P. Xue, L. L. Shan, H. Y. Chen, Y. Li, H. Y. Zhu, D. W. Deng, Z. Y. Qian, S. Achilefu and Y. Q. Gu, *Biosens. Bioelectron.*, 2013, **41**, 71-77;

(c) N. Li, C. Y. Chang, W. Pan and B. Tang, *Angew Chem Int Edit*, 2012, **51**, 7426-7430.
19. (a) Y. P. Kim, Y. H. Oh, E. Oh, S. Ko, M. K. Han and H. S. Kim, *Anal. Chem.*, 2008, **80**, 4634-4641; (b) D. W. Deng, D. Y. Zhang, Y. Li, S. Achilefu and Y. Q. Gu, *Biosens. Bioelectron.*, 2013, **49**, 216-221.
20. (a) D. Zheng, D. S. Seferos, D. A. Giljohann, P. C. Patel and C. A. Mirkin, *Nano Lett.*, 2009, **9**, 3258-3261; (b) X. Y. Huang, T. Lan, B. C. Zhang and J. C. Ren, *Analyst*, 2012, **137**, 3659-3666.
21. J. J. Schmidt and K. A. Bostian, *J. Protein Chem.*, 1997, **16**, 19-26.
22. X. Liu, Y. Wang, P. Chen, Y. Wang, J. Zhang, D. Aili and B. Liedberg, *Anal. Chem.*, 2014, DOI: 10.1021/ac402626g.
23. J. J. Schmidt and K. A. Bostian, *J. Protein Chem.*, 1995, **14**, 703-708.
24. P. Chen, R. Selegard, D. Aili and B. Liedberg, *Nanoscale*, 2013, **5**, 8973-8976.
25. S. Link and M. A. El-Sayed, *Int. Rev. Phys. Chem.*, 2000, **19**, 409-453.
26. R. Kukreja and B. R. Singh, in *Microbial Toxins: Current Research and Future Trends*, Caister Academic Press., 2009.
27. G. S. Coombs, M. S. Rao, A. J. Olson, P. E. Dawson and E. L. Madison, *J. Biol. Chem.*, 1999, **274**, 24074-24079.
28. R. M. Caprioli and L. Smith, *Anal. Chem.*, 1986, **58**, 1080-1083.
29. X. Michalet, S. Weiss and M. Jager, *Chem. Rev.*, 2006, **106**, 1785-1813.
30. F. Wei and C. M. Ho, *Anal. Bioanal. Chem.*, 2009, **393**, 1943-1948.
31. K. E. Sapsford, J. Granek, J. R. Deschamps, K. Boeneman, J. B. Blanco-Canosa, P. E. Dawson, K. Susumu, M. H. Stewart and I. L. Medintz, *ACS Nano*, 2011, **5**, 2687-2699.
32. M. Lindstrom and H. Korkeala, *Clin. Microbiol. Rev.*, 2006, **19**, 298-+.

